

Received: 15 May 2013 – Accepted: 24 May 2013 – Published: 7 June 2013

Correspondence to: N. R. Nowaczyk (norbert.nowaczyk@gfz-potsdam.de)

Published by Copernicus Publications on behalf of the European Geosciences Union.

CPD

9, 3061–3102, 2013

Chronology of Lake El'gygytgyn sediments

N. R. Nowaczyk et al.

Title Page

Abstract

Introduction

Conclusions

References

Tables

Figures



Back

Close

Full Screen / Esc

Printer-friendly Version

Interactive Discussion



Abstract

A 318 m long sedimentary profile drilled by the International Continental Scientific Drilling Program (ICDP) at Site 5011-1 in Lake El'gygytyn, Far East Russian Arctic, has been analysed for its sedimentologic response to global climate modes by chrono-stratigraphic methods. The 12 km wide lake is sited in an 18 km large crater that was created by the impact of a meteorite 3.58 Ma ago. Since then sediments have been continuously deposited. For establishing their chronology, major reversals of the Earth's magnetic field provided initial tie points for the age model, confirming that the impact occurred in the earliest Gauss chron. Various stratigraphic parameters, reflecting redox conditions at the lake floor and climatic conditions in the catchment were tuned synchronously to Northern Hemisphere insolation variations and the marine oxygen isotope stack, respectively. Thus, a robust age model comprising more than 600 tie points could be defined. It could be shown that deposition of sediments in Lake El'gygytyn occurred in concert with global climatic cycles. The upper ~ 160 m of sediments represent the past 3.3 Ma, equivalent to sedimentation rates of 4 to 5 cm ka⁻¹, whereas the lower 160 m represent just the first 0.3 Ma after the impact, equivalent to sedimentation rates in the order of 45 cm ka⁻¹.

1 Introduction

Lake El'gygytyn in the Far East Russian Arctic (67.5° N, 172° E) with a diameter of 12 km is located in an 18 km wide impact crater formed 3.58 Ma ago (Layer, 2000). The 170 m deep lake has a bowl-shaped morphology, a surface area of 110 km², and a relatively small catchment of 293 km² (Nolan and Brigham-Grette, 2007). The bedrock in the crater catchment consist mainly of igneous rocks, lava, tuffs, ignimbrites of rhyolites and dacites, rarely andesites and andesitic tuffs (Gurov and Koeberl, 2004), some of them having ages from 83.2 to 89.3 Ma (Layer, 2000) and 88 Ma (Keeley et al., 1999). Thus, they were emplaced during the Cretaceous normal polarity super-chron (Ogg

Chronology of Lake El'gygytyn sediments

N. R. Nowaczyk et al.

Title Page

Abstract

Introduction

Conclusions

References

Tables

Figures



Back

Close

Full Screen / Esc

Printer-friendly Version

Interactive Discussion



Chronology of Lake El'gygytyn sediments

N. R. Nowaczyk et al.

Title Page

Abstract

Introduction

Conclusions

References

Tables

Figures



Back

Close

Full Screen / Esc

Printer-friendly Version

Interactive Discussion



algae such as *Chlamidomonas*) in the water body. From mid-autumn to mid-spring all these processes come to a standstill. Thus, not just the intensity of insolation but also the length of the summer appears to be important. Therefore, we used the cumulative summer insolation from May to August for tuning. Obtained variations in tree and shrub pollen percentage and biogenic silica (BSi) represent vegetational conditions in the (wider) area around the lake and bioproductivity within its water body, respectively. Sediment grain size, spectral colour, titanium (Ti) content, and Si/Ti-ratio, the latter two parameters obtained from X-ray fluorescence (XRF) scanning, reflect mostly weathering and transport processes within and from the catchment, respectively, which in turn depend on climatic conditions. After first age assignments using magnetic polarity stratigraphy, all these parameters together show striking similarities to global climate variability as expressed by the LR04 stack (Lisiecki and Raymo, 2005), which was therefore taken as reference curve. The major environmental implications of the El'gygytyn paleoclimate record, occurrence of "super-interglacials" and the stepwise cooling of the Northern Hemisphere are discussed in Melles et al. (2012) and Brigham-Grette et al. (2013), respectively.

In general, age models derived from tuning include several problems, such as circular reasoning or chronological uncertainties in both the reference record and the record to be tuned, when only restricted sets of data are consulted (Blaauw 2012). However, wiggle matching can be further validated by using multi-proxy tuning (e.g. Bokhorst and Vandenberg, 2009; Prokopenko et al., 2006), as it was also performed in this study.

2 Material and methods

2.1 Data acquisition

For magnetostratigraphic investigation the upper about 140 m of sediments were continuously subsampled with U-channels, whereas the remaining sequences were nearly exclusively analysed by using discrete samples, due to increasing stiffness

of the sediments. Defining the inclination of characteristic remanent magnetization (ChRM), providing polarity for interpretation, is based on principle component analysis (Kirschvink, 1980) of results from stepwise and complete alternating field demagnetisation of all material. Further information on sampling strategy, data acquisition techniques, and methods of processing are given by Haltia and Nowaczyk (2013).

Magnetic (volume) susceptibility from cores PG1351 and Lz1024 were acquired with a Bartington MS2E sensor in combination with a MS2 control unit, integrated into the 1st generation GFZ split-core logger (scl-1.1). Magnetic susceptibility and colour information from sediments from ICDP Site 5011-1 cores were obtained every 1 mm using a 2nd generation split-core logger (scl-2.3), with its hard- and software designed and built at the Helmholtz Centre Potsdam, GFZ. Magnetic susceptibility was measured with a Bartington MS2E spot-reading sensor first attached to a MS2 control unit, which was later replaced by a technically improved MS3 control unit.

The response function of the MS2E sensor with respect to a thin magnetic layer is equivalent to a Gaussian curve with a half-width of slightly less than 4 mm (e.g. Fig. 4 in Nowaczyk, 2001). The amplitude resolution of the sensor is 10×10^{-6} in combination with the MS2 unit and 2×10^{-6} with the improved MS3 unit, both using an integration time of about a second. During data acquisition, after every 10 measurements, the sensor is lifted about 4 cm above the sediment in order to take a blank reading against air. This is done in order to monitor the shift of the sensor's background due to temperature drift. Subsequently, the air readings were linearly interpolated and subtracted from the readings on sediment.

A spectrophotometer (GretagMacbeth SpectrolinoTM) was applied with the scl-2.3 logger for acquiring a full colour spectrum from 380 to 720 nm at a physical resolution of 10 nm, that is, providing 36 spectral lines for each measuring spot from ICDP Site 5011-1 cores. For sediments recovered within cores PG1351 and Lz1024 no colour information is available. The spectrophotometer integrates over a circular window of 4 mm in diameter (centre-weighted). In addition to the visible spectrum further colour information, derived from the spectral data, was transmitted by the instrument: the tristimulus

Chronology of Lake El'gygytyn sediments

N. R. Nowaczyk et al.

[Title Page](#)[Abstract](#)[Introduction](#)[Conclusions](#)[References](#)[Tables](#)[Figures](#)[Back](#)[Close](#)[Full Screen / Esc](#)[Printer-friendly Version](#)[Interactive Discussion](#)

Chronology of Lake El'gygytyn sediments

N. R. Nowaczyk et al.

Title Page

Abstract

Introduction

Conclusions

References

Tables

Figures



Back

Close

Full Screen / Esc

Printer-friendly Version

Interactive Discussion



values (X,Y,Z), defined by the International Commission on Illumination (CIE) in 1931, and vectors in the 1976 CIE (L^* , a^* , b^*) colour space. The tristimulus values of a colour are the amounts of the three colours the human eye can perceive (red, green, blue) in a three-component additive colour model (Fig. 2a). However, in order to reproduce a measured colour represented by (X,Y,Z), e.g. on a TV or computer screen, a 3×3 matrix has to be applied to the (X,Y,Z) vector in order to obtain the required (R,G,B) values for display, as it is implemented in the split-core logger's controlling computer program. The elements of the matrix depend on type of illumination and observing angle, as well as on the (R,G,B) properties of the used hardware and/or computer operating system (or television system).

In the (L^* , a^* , b^*) colour space (Fig. 2b), the a^* coordinate represents variations in colour between red ($a^* > 0$) and green ($a^* < 0$), whereas the b^* coordinate represents variations in colour between yellow ($b^* > 0$) and blue ($b^* < 0$). The L^* component represents lightness (0 = black, 100 = white). In order to distinguish major colour changes of the sediments from Lake El'gygytyn the hue angle (H) was also determined (Fig. 2b, c). It is calculated as $H = \text{atan2}(b^*, a^*)$, with $0^\circ \leq H \leq 360^\circ$. Hue values of major colours are: red = $0^\circ/360^\circ$, yellow = 60° , green = 120° , cyan = 180° , blue = 240° , magenta = 300° . An example of sediment color, hue angle distribution, and individual color spectra as obtained with the SpectrolinoTM is shown in Fig. 3.

Since both the susceptibility and colour sensors need to be in full contact to the sediment surface, the scl-2.3 logger is additionally equipped with a third sensor, a high-precision mechanical micro-switch to scan the surface morphology first. This is achieved by moving the switch from a certain reference height downward onto the sediment where the switch triggers the termination of its own movement. Triggering force is in the range of 5 gram. The distance moved by the switch is determined by the stepping motor control, thus supplying the information needed for subsequently lowering the susceptibility sensor and the spectrophotometer onto the sediment for data acquisition. During data acquisition core segments were covered by a thin and clear plastic foil in order to prevent all three sensors from being stained by the soft and moist

sediments. Ideally, the foil is completely free of air bubbles and clinging to the sediment surface due to sediment moisture. However, the older the sediments are the lower their moisture content is. Thus, downward from about 200 m on, the foil was not always completely attached to the sediments and colour information got slightly biased with increasing drilling depth.

2.2 Further data used for tuning

Biogenic silica (BSi) contents were estimated at a sampling interval of 20 mm by using Fourier transform infrared spectroscopy (FTIRS). The method is described in detail by Vogel et al. (2008) and Rosén et al. (2010, 2011). Biogenic silica is mostly derived from diatoms, which are the major contributors to the intra-lake bioproduction (e.g. Cherapanova et al., 2007). Post sedimentary dissolution of diatom frustules is negligible in sediments of Lake El'gygytyn. Thus, the percentage of biogenic silica is taken as a proxy for bioproductivity in Lake El'gygytyn. A detailed discussion on FTIRS results from ICDP Site 5011-1 is provided by Meyer-Jacob et al. (2013) and Vogel et al. (2012).

The content of total organic carbon (TOC) was determined every 20 mm using a Vario microCube elemental analyzer (Elementar, Germany). Elemental scans of major elements were performed with an ITRAX XRF (X-ray fluorescence) core scanner (Cox Analytical, Sweden), equipped with Cr- and Mo-tubes, respectively, which were set to 30 kV and 30 mA. The abundance of elements was determined at 2 mm resolution with an integration time of 10 s per measurement. The relative abundance of titanium (Ti) is taken as a proxy of clastic lithogenic input, whereas silica (Si) represents the sum of both lithogenic and biogenic Si. Thus, the Si/Ti-ratio reflects the variable contribution of biogenic silica against the clastic lithogenic background. For further details see Wenrich et al. (2013). Grain-size variability was estimated by principle component analysis (PCA) of granulometric analyses using a laser particle analyzer (Francke et al., 2013). For tuning of the ICDP Site 5011-1 composite record PC 1 (principle component 1) was used, with negative (positive) values representing coarse (fine) grained sediments.

Chronology of Lake El'gygytyn sediments

N. R. Nowaczyk et al.

Title Page

Abstract

Introduction

Conclusions

References

Tables

Figures



Back

Close

Full Screen / Esc

Printer-friendly Version

Interactive Discussion



Pollen data is available every 8 cm, with lower resolution in the Pliocene section (see also Andreev et al., 2013; Lozhkin and Andersen, 2013). Where available, the percentage of tree and shrub pollen was used as an additional environmental indicator with high (low) percentages representing warm (cold) conditions. Data from PG1351 are from Nowaczyk et al. (2002), data from Lz1024 are from Lozhkin et al. (2007).

2.3 Creation of a composite

For analysis of the Lake El'gygytgyn sedimentary succession a composite was created using data from core Lz1024, recovered in 2003, and from ICDP Site 5011-1, comprising only partly overlapping holes 1A, 1B, and 1C, recovered in 2009. From the 16.64 m long core Lz1024 data records of the upper 5.67 m were used to supplement the uppermost section of the composite that was not recovered with ICDP Site 5011-1 cores. According to initial data analysis, this depth interval is equivalent to marine oxygen isotope stages (MIS) 1 to 4 and most of MIS 5 (back to about 125 ka). Below 5.67 m, and until about 104.8 m composite depth, alternating sediment intervals from parallel holes 5011-1A and 1B were spliced together. Between 104.8 and 113.4 m composite depth additional information from core 5011-1C could be used. Between 113.4 and 145.7 m composite depth, cores 1A and 1C contributed to the composite. Below 145.7 m composite depth down to the sediment impact breccia interface at 318 m, only core 5011-1C, which has a mean recovery rate of only 50 % (Melles et al., 2011), could be used. However, at least the lowermost 38 m of the composite (280 to 318 m) is available with 90 to 99 % recovery.

Core intervals for the composite were selected mainly by visual inspection, using the better preserved/least disturbed sections from one of the records in cases of overlapping recovery. In general, tephra layers, turbidites, and mass movements were omitted leaving gaps within the composite data sets. Further details are described by Wennrich et al. (2013).

Chronology of Lake El'gygytgyn sediments

N. R. Nowaczyk et al.

Title Page

Abstract

Introduction

Conclusions

References

Tables

Figures



Back

Close

Full Screen / Esc

Printer-friendly Version

Interactive Discussion



2.4 Tuning

Fixed tie points for the ICDP Site 5011-1 composite record are provided by magnetostratigraphic investigation of sediments from this site by Haltia and Nowaczyk (2013). Ages for the documented major reversals were mainly assigned according to Lisiecki and Raymo (2005) as listed in Table 1. Between the tie points provided by magnetostratigraphy, a synchronous tuning of nine additional data sets was performed using an interactive wiggle matching software. The extended tool for correlation (**xtc**, Linux-based) is capable of loading all necessary data sets together into the memory of the computer (down-core data sets, reference data sets, age models, positions of tephras, scaling of axes). The (partly huge) sizes of the data sets used for tuning are listed in Table 2. 1 mm spot-readings of magnetic susceptibility and TOC data, determined every 10 to 20 mm, were tuned to the Northern Hemisphere (67.5° N, El'gygytyn latitude) cumulative spring/summer insolation (May to August) according to Laskar et al. (2004). Parallel to this, Ti as well as Si/Ti ratios based on 2 mm readings of X-ray fluorescence (XRF) counts, percentages of biogenic silica (BSi, opal) derived from Fourier transform infrared spectroscopy (FTIRS), determined every 20 mm, the hue angle determined every 1 mm, grain size PCA data, and tree pollen percentages were tuned to the LR04 marine oxygen isotope stack of Lisiecki and Raymo (2005). Jointly to the tuning of the ICDP Site 5011-1 data sets, age models for the Lake El'gygytyn pilot cores were also developed (Lz1024) and refined (PG1351), respectively.

3 Results

It was intended to provide a sedimentary paleoclimatic proxy-record that is cleaned from tephra layers, turbidites, slumps, and other disturbances, such as observed folded sediments. Therefore, such intervals were discarded for the creation of the ICDP Site 5011-1 composite. However, such sediment intervals can still provide useful information at least on the polarity of the geomagnetic field during their deposition. The

CPD

9, 3061–3102, 2013

Chronology of Lake El'gygytyn sediments

N. R. Nowaczyk et al.

Title Page

Abstract

Introduction

Conclusions

References

Tables

Figures



Back

Close

Full Screen / Esc

Printer-friendly Version

Interactive Discussion



expected dipole inclination for the site of Lake El'gygytyn is 78.3° . Thus, folded layers with a tilt of 45° will still yield positive (negative) inclination during normal (reversed) polarity. It then depends on the angle between magnetization direction and tilting direction whether the disturbed direction is shallower or steeper than the undisturbed one.

Also turbidites, although representing short depositional events on a geological time scale, should record a proper polarity if not even a proper direction at least in their upper fine-grained section. Therefore, in intervals close to reversals, the directional data of rejected intervals, such as the onset of the Olduvai subchron and reversals within the Gauss chron (see Haltia and Nowaczyk, 2013), were also taken into consideration when determining the polarity and localization of the major reversals.

3.1 Iterative tuning

The general strategy of tuning is exemplarily demonstrated by data covering the time window from 740 to 1000 ka, comprising the Brunhes Matuyama reversal as well as the termination of the Jaramillo subchron (Fig. 4). Note that for reasons of clarity not all resulting correlation tie points within this interval are displayed. The major reversals of the Earth's magnetic field, as incorporated in the official geomagnetic polarity time scale (GPTS, Ogg and Smith, 2004; Table 1), provide twelve 1st order tie points (red dotted lines in Fig. 4) during the last 3.6 Ma for the age model, from which ten are very well defined in the El'gygytyn sedimentary sequence. Only the top of Kaena and the base of Mammoth subchrons, both within the Gauss chron, are somewhat ambiguous, when only (cleaned) paleomagnetic information are considered. To further 1st order tie points could be derived from the short-termed Cobb Mountain event (Mankinen et al., 1978) within the Matuyama Chron, clearly linked to MIS 35 (Channell et al., 2008). Figure 4 comprises the Brunhes Matuyama reversal and the termination of the Jaramillo subchron as 1st order tie points. For the base of the lacustrine sediment section from Lake El'gygytyn the age of the impact of 3.58 ± 0.04 Ma was adopted from Layer (2000) as another 1st order tie point.

Chronology of Lake El'gygytyn sediments

N. R. Nowaczyk et al.

Title Page

Abstract

Introduction

Conclusions

References

Tables

Figures



Back

Close

Full Screen / Esc

Printer-friendly Version

Interactive Discussion



Chronology of Lake El'gygytyn sediments

N. R. Nowaczyk et al.

Title Page

Abstract

Introduction

Conclusions

References

Tables

Figures



Back

Close

Full Screen / Esc

Printer-friendly Version

Interactive Discussion



After adopting this approach to convert depths into ages it became obvious that the morphology of the log(Si/Ti-ratio) curve obtained from XRF scanning resembles the LR04 oxygen isotope reference curve from Lisiecki and Raymo (2005) quite well (Fig. 4b, d). The same is valid for the Ti content and the hue angle, when both plotted on an inverse axis (not shown in Fig. 4), and partly the record of biogenic silica, obtained from Fourier transform infrared spectroscopy (FTIRS-BSi), which mainly resembles the peak warm interglacials from above a certain threshold level (Fig. 4a). This set of proxy records therefore was used to define 2nd order tie points (dark green short-dashed lines in Fig. 4) by interactive wigggle matching to the LR04 curve.

Compared to the LR04 stack, the Northern Hemisphere summer insolation shows a much stronger variability. Note that already the onsets of interglacials, MIS 19, 21, and 25, are linked to pronounced insolation maxima. In the further course of these interglacials one (MIS 19 and 25) or even two local insolation minima occur (MIS 21). These local minima and most of all other minima in insolation are obviously linked to lows in magnetic susceptibility and highs in TOC when applying 1st and 2nd order tie points for correlation. To be more precise, the bases of many sediment intervals characterized by low magnetic susceptibility and high values of TOC generally coincide with minima in insolation. The top of these intervals coincide fairly well with the steepest gradient of increasing insolation after the preceding insolation minimum, and the base of intervals characterized by high susceptibility are linked to insolation maxima. Thus, 3rd order tie points could be defined for fine-tuning (blue long-dashed lines in Fig. 4). However, there are additional TOC peaks related to certain interglacials which are also characterized by exceptional high biogenic silica values and high Si/Ti-ratios, such as MIS 5, 9, 11, 17, 25 (see Fig. 4), 31, 47, and 49. In these cases the TOC values are mostly controlled by a high primary bio-production and a better preservation due to fast oxygen consumption and hampered degradation in the uppermost sediment succession. Magnetic susceptibility values in these intervals are one order of magnitude higher than those from anoxic intervals. This points towards at least sub-oxic bottom water conditions and implies that at least partial degradation of organic matter should

have occurred so that the associated TOC peaks very likely give an underestimation of the primary bioproductivity (Nowaczyk et al., 2002, 2007). The other TOC peaks (note that TOC is plotted on an inverted axis) are associated with minima in Si/Ti ratios, indicating low bioproductivity. Thus, these intervals represent just phases of less efficient degradation of organic matter under sub-oxic bottom water conditions. These types of conditions are in turn the least favourable for magnetite preservation leading to the observed lows in magnetic susceptibility (Nowaczyk et al., 2002, 2007).

3.2 Chronostratigraphy and precision of age model

Figure 5 shows the most important parameters from ICDP Site 5011-1 composite record after synchronous tuning to the GPTS, the LR04 stack, and the Northern Hemisphere summer insolation, respectively. The parameters that were mainly tuned to the LR04 marine oxygen isotope stack (Fig. 5f), are plotted in the left section (Fig. 5a to e): grain size variations, hue angle (sediment colour), biogenic silica (FTIRS-BSi), Si/Ti-ratio from XRF-scanning, and tree and shrub pollen percentages, where available, including results from pilot cores PG1351 and Lz1024. The ChRM inclinations of the ICDP Site 5011-1 composite record (Fig. 5g), is plotted to the right of the LR04 stack. Geomagnetic field reversals can be recognized from flips between steep positive inclinations (normal polarity, grey background) and steep negative inclinations (reversed polarity, white background). Thus, the ICDP Site 5011-1 sedimentary record comprises the three geomagnetic chrons including Brunhes, Matuyama, and (most of the) Gauss, that is, the last about 3.6 Ma. The right section of Fig.5 relates variations of total organic carbon (TOC, Fig. 5h) and magnetic susceptibility (Fig. 5i) to the Northern Hemisphere insolation (cumulative, May to August, 67.5° N, Fig. 5j). The obtained age model of the ICDP 5011 composite is shown in Fig. 6 and age models for the pilot cores, PG1351 and Lz1024, are shown in Fig. 7. Mean sedimentation rates in Lake El'gygytgyn are in the range of 4 cmka⁻¹ for the last about 1.0 Ma. Going further back in time, sedimentation rates slightly increase to about 5 cmka⁻¹ between 2.5 and 3.0 Ma, whereas the interval between 3.3 and 3.6 Ma is characterized by ten-fold higher sedimentation

Chronology of Lake El'gygytgyn sediments

N. R. Nowaczyk et al.

Title Page

Abstract

Introduction

Conclusions

References

Tables

Figures



Back

Close

Full Screen / Esc

Printer-friendly Version

Interactive Discussion



rates of about 45 cm ka^{-1} . This must be due to major environmental changes. In the marine LR04 oxygen isotope stack the oldest shift towards heavier values during the past 3.6 Ma, MIS M2 within the early Mammoth subchron, occurs around 3.3 Ma (see Supplement for a more detailed display and labelling of data). This is paralleled by a drastic drop in tree and shrub pollen percentage down to 20% in the sedimentary record of Lake El'gygytgyn. Furthermore, this actually substantiated the position of the onset of the Mammoth subchron in the ICDP Site 5011-1 record, since here the interpretation of paleomagnetic data is hampered by numerous recovery gaps and low core quality.

In the first place, the precision of the age model(s) of Lake El'gygytgyn sediments is limited by the accuracy, precision and temporal resolution of the reference curves. The LR04 oxygen isotope stack for the last 5 Ma is provided in 1 kyr increments. Lisiecki and Raymo (2009) point out that especially the timing of glacial terminations documented in benthic oxygen isotope records from the Atlantic and the Pacific can already differ by up to 4 kyr. This problem accounts mainly for new marine benthic oxygen isotope records to be dated by correlation to a master record. However, the LR04 stack/master record is based on records with a global distribution, including the Atlantic and Pacific Oceans, so that stratigraphic correlation to it might introduce inaccuracies in dating in the range of several kyrs. The LR04 stack has been tuned to the 21 June insolation at 65° N according to orbital solutions of Laskar et al. (1993). Because of uncertainties in these solutions Lisiecki and Raymo (2005) conclude that absolute ages in their LR04 stack might be offset by several kyrs, depending on time interval: up to 4 kyr from 0–1 Ma, up to 6 kyr from 1–3 Ma, up to 15 kyr from 3–4 Ma.

In addition to usage of the LR04 stack as stratigraphic reference we tuned magnetic susceptibility and TOC variations from Lake El'gygytgyn sediments to updated orbital solutions given in increments of 0.25 kyr and with an uncertainty of 0.1% according to Laskar et al. (2004). Thus, tuning data with ages around 3 Ma might be offset by only 3 kyr. Therefore, absolute ages of El'gygytgyn sediments are possibly offset by up to about 3 kyr (considering Laskar et al., 2004) to 15 kyr (considering Lisiecki and

Chronology of Lake El'gygytgyn sediments

N. R. Nowaczyk et al.

[Title Page](#)[Abstract](#)[Introduction](#)[Conclusions](#)[References](#)[Tables](#)[Figures](#)[Back](#)[Close](#)[Full Screen / Esc](#)[Printer-friendly Version](#)[Interactive Discussion](#)

Raymo, 2005) in the Pliocene, but relative age assignments to the reference records should have a precision of some 500 yr since many (3rd order) tie points were derived from the insolation reference record, which has a higher temporal resolution.

4 Discussion

4.1 Age of meteorite impact

The lowermost distinctly stratified sediments recovered from Lake Elgygytyn clearly show normal polarity. Some intercalations of suevitic material in this section imply that these sediments must have been deposited shortly after the impact. The suevites are supposed to have been episodically washed in from the intra-crater catchment. Paleomagnetic data from the underlying suevites show predominantly a normal polarity, too (Maharaj et al., 2012). Thus, it can be concluded, that the impact that created the El'gygytyn Crater occurred definitely after the Gauss-Gilbert reversal (Table 1). However, it is not clear how long it took to form a permanent lake within the impact crater. Figure 8 shows the dating of the impact by Layer (2000) within the context of the geomagnetic polarity time scale(s). The 1σ error range of the dating (3.58 ± 0.04 Ma) crosses the Gauss Gilbert reversal. Thus, the only conclusion that can be drawn is that the older (upper) limit for the age of the impact can be set to 3.588 Ma, when adopting the LR04 time scale, or, to 3.596 Ma when using the Ogg and Smith (2004) GPTS. Unfortunately, no biogenic remnants (neither diatoms, nor pollen) that would allow assignments to climate cycles are preserved within the lowermost about 25 m of sediments. Therefore, the younger (lower) limit of the impact age of 3.540 Ma is still defined by the 1σ error range of Layer (2000).

4.2 Polarity stratigraphy

In general, as listed in Table 1, our multi-proxy study of the Lake El'gygytyn ICDP Site 5011-1 sedimentary record confirms ages of geomagnetic reversals within the

Chronology of Lake El'gygytyn sediments

N. R. Nowaczyk et al.

Title Page

Abstract

Introduction

Conclusions

References

Tables

Figures



Back

Close

Full Screen / Esc

Printer-friendly Version

Interactive Discussion



past 3.6 Ma as given by Lisiecki and Raymo (2005). Table 1 lists also ages of known reversals provided in the geomagnetic polarity times scales (GPTS) of Cande and Kent (1995), Lourens et al. (1996), and Ogg and Smith (2004), since Lisiecki and Raymo (2005) do not provide ages for all of them. In addition to this, reversal ages listed in the various GPTSs slightly deviate from each other.

Paleomagnetic data quality of the Gauss chron at ICDP Site 5011-1 is very heterogeneous since it is based mainly on a single core, ICDP Site 5011-1C (Haltia and Nowaczyk, 2013). Normal polarity in its earliest part is very well established. But, between ~ 3.55 and ~ 2.95 Ma (290 and 145 m composite depth) directions are fairly scattered due to numerous recovery gaps and bad core quality, with at least some increase of data coverage around the middle Gauss normal polarity phase. Thus, the onset of the Mammoth and the termination of the Kaena reversed polarity subchrons are not clearly expressed. However, using the available data set of climate-proxy parameters a fairly robust age model could be achieved even for this interval. From ~ 2.95 Ma on (290 m composite depth) the ICDP Site 5011-1 composite is based on at least two cores and normal polarity within the upper Gauss chron is well expressed.

According to our study, the Matuyama Gauss reversal, consistently documented in cores ICDP Site 5011-1A and 1C (Haltia and Nowaczyk, 2013), occurred at 2.588 Ma, clearly within MIS 103 (Table 1, Fig. 5). Deino et al. (2006) provide an $^{40}\text{Ar}/^{39}\text{Ar}$ -based age of 2.589 ± 0.003 Ma from two tephtras, tightly bracketing the Matuyama Gauss reversal in the upper part of a diatomite of the fluvio-lacustrine sediments in the Chemeron Basin, Central Kenya Rift, Afrika. This would be in excellent agreement to our result. However, Deino et al. (2006) tune their radiometrically obtained age to an astronomically polarity time scale and shift this age to 2.610 Ma. This is close to the age of 2.608 Ma, given by Lisiecki and Raymo (2005). But, this would place the Matuyama Gauss reversal into MIS 104, a cold interval. This contradicts our stratigraphic results that only **allow to place the** Matuyama Gauss reversal into the middle MIS 103 (Table 1, Fig. 5), that is, within a warm interval. This is also in agreement with findings by Prokopenko and Khursevich (2010) from Lake Baikal site BDP-96. Thus,

Chronology of Lake El'gygytyn sediments

N. R. Nowaczyk et al.

[Title Page](#)[Abstract](#)[Introduction](#)[Conclusions](#)[References](#)[Tables](#)[Figures](#)[Back](#)[Close](#)[Full Screen / Esc](#)[Printer-friendly Version](#)[Interactive Discussion](#)

Chronology of Lake El'gygytyn sediments

N. R. Nowaczyk et al.

Title Page

Abstract

Introduction

Conclusions

References

Tables

Figures



Back

Close

Full Screen / Esc

Printer-friendly Version

Interactive Discussion



of magnetic particles can be assumed during dominating oxic conditions at the lake floor. However, in most cases the MS curve lies below the Ti curve, indicating far-reaching dissolution of up to 95% of the magnetic fraction. There is even an anti-correlation between Ti content and magnetic susceptibility visible during longer sequences within the El'gygytyn sedimentary record. Thus, magnetic susceptibility is **everything** but a proxy for the input of lithogenic material, although magnetic particles were very likely derived from the catchment inside the El'gygytyn crater, bearing highly magnetic volcanic rocks. The massive loss of magnetic particles of up to 95% still **allowed a save determination of** geomagnetic reversals (Haltia and Nowaczyk, 2013), but it definitely excludes a reliable estimation of relative geomagnetic paleointensity variations (Nowaczyk et al., 2002, 2007). This is a major deficit of the El'gygytyn sedimentary record, because correlation of paleointensity variations to reference records, such as the PISO1500 stack (Channell et al., 2009) or the EPAPIS-3000 stack (Yamazaki and Oda, 2005, and further references therein), could have provided further geomagnetic tie points between the major reversals. This could have significantly substantiated the age model mainly derived from tuning Lake-El'gygytyn sedimentary climate-proxies to the LR04 stack (Lisiecki and Raymo, 2005) and the Northern Hemisphere cumulative summer insolation, according to orbital solutions by Laskar et al. (2004). On the other hand, only the strict link between alternating redox conditions, leading to the alternating dissolution/preservation effects described above, and insolation variations enabled the definition of many tie points in the age model for ICDP Site 5011-1. Figure 9b also shows a clear anti-correlation between Ti and the LR04 stack. This indicates a dilution of the lithogenic fraction by biogenic components being larger (smaller) during warm (cold) phases. A good proxy for the varying ratio of bioproductivity, in Lake El'gygytyn mostly biogenic (bio) silica from diatoms, to lithogenic (litho) input is the Si/Ti-ratio (Melles et al., 2012; Wennrich et al., 2013), here obtained in high-resolution from XRF-scanning (Fig. 9c). Actually this ratio is $(Si_{\text{bio}} + Si_{\text{litho}})/Ti_{\text{litho}}$. Thus, when Si_{bio} approximates zero the Si/Ti-ratio approximates a certain value, depending on the average composition of the catchment rocks. The pure $(Si/Ti)_{\text{litho}}$ -ratio might also change

Chronology of Lake El'gygytyn sediments

N. R. Nowaczyk et al.

Title Page

Abstract

Introduction

Conclusions

References

Tables

Figures



Back

Close

Full Screen / Esc

Printer-friendly Version

Interactive Discussion



due to an increased (decreased) chemical alteration under anoxic (oxic) condition in cold (warm) phases at the lake floor (Minyuk et al., 2007). Nevertheless, the modulation of the Si/Ti-ratio is obviously dominated by its varying biogenic contribution since the Si/Ti-ratio resembles strongly the morphology of the biogenic silica (FTIRS-BSi) curve (Fig. 5). The variations in Si/Ti-ratio are also paralleled by changes in colour (hue angle) from yellowish brown (80°) to greenish grey (140°), also shown in Fig. 9c. Up to now, these color changes have not been investigated in detail, but probably they represent the alternation between predominantly chemical and physical alteration, as proposed by Minyuk et al. (2007), in concert with climatic variations (Fig. 9c). Anyhow, the hue angle turned out to be a very helpful parameter for tuning the ICDP Site 5011-1 sedimentary sequence and more detailed analyses of the full spectral colour information, from which the hue angle was derived, might give further information in the future. The percentages of tree & shrub pollen also vary in concert with variation in biogenic silica, Si/Ti-ratio, color (hue), and grain size (Fig. 5), but these aspects exceed the focus of this paper. Major environmental implications of the pollen record is published in Melles et al. (2012) and Brigham-Grette et al. (2013).

4.4 Tephra layers

Up to now, a total of eight tephra layers have been identified in Lake El'gygytyn sediments. Currently, radiometric ages are not yet available. However, based on multi-proxy tuning of the sediments they are embedded in, tephra ages could be determined by chrono-stratigraphic means. Their positions in composite depth and respective ages are listed in Table 3. Work on the geochemical fingerprints of the tephra layers is in progress.

5 Conclusions

Despite the presence of more than 300 turbidites, mass movements of up to 1.2 m thickness (Sauerbrey et al., 2013), and **bad** core recovery in the lower section, a fairly detailed age model could be achieved for the about 320 m thick ICDP Site 5011-1 sedimentary composite record from Lake El'gygytgyn, Far Eastern Russian Arctic, covering the past 3.6 Ma. Reference ages of 14 reversals of the geomagnetic field, documented in the sediments, are provided by the time scales of Lisiecki and Raymo (2005) and Ogg and Smith (2004), respectively, showing slightly deviating ages for some of the reversals (Table 1). Within that range, reversal ages derived from chronostratigraphic analyses of Lake El'gygytgyn sediments are in a general agreement with these time scales. Thus, we suggest an age of 2.588 Ma for the Matuyama Gauss reversal. For the Réunion subchron a duration extending from 2.1216 to 2.1384 Ma could be derived. Our study confirms the existence of a short-term Olduvai precursor from 1.9815 to 1.9782 Ma, reaching full normal polarity, also documented in North Atlantic sediments (Channell et al., 2003). In ICDP Site 5011-1 sediments, the Cobb Mountain subchron is covering the time interval from 1.1938 to 1.1858 Ma. Our data also give evidence for an intra-Jaramillo excursion lasting from 1.0192 to 1.0142 Ma in MIS 29, which is younger than ages derived from other studies placing it in MIS 30 (Channell et al., 2002). Despite recording of such short-term geomagnetic field features during the Matuyama chron no evidence for excursions within the Brunhes chron was found in Lake El'gygytgyn sediments and repeatedly occurring pervasive magnetite dissolution throughout the whole Pleistocene inhibited a reconstruction of paleointensity variations. Nevertheless, in addition to the polarity stratigraphy, a synchronous tuning of 9 stratigraphic parameters to the LR04 marine oxygen isotope stack (Lisiecki and Raymo, 2005) and to the Northern Hemisphere cumulative summer insolation (May to August), according to orbital solution by Laskar et al. (2004), respectively, led to a significant refinement of the age model by the definition of a total of about 600 tie points. The age model has some uncertainties towards the base of the (Pliocene) sediments

Chronology of Lake El'gygytgyn sediments

N. R. Nowaczyk et al.

Title Page

Abstract

Introduction

Conclusions

References

Tables

Figures



Back

Close

Full Screen / Esc

Printer-friendly Version

Interactive Discussion



between 2.94 and 3.54 Ma, mainly due to low sediment recovery during drilling. Here, pronounced variation in the percentages of tree pollen provided major clues for age assignments. Estimated sedimentation rates are in the range of 4 to 5 cm ka⁻¹ for the past about 3.3 Ma, whereas the first 0.3 Ma after the impact that created the El'gygytyn crater are characterised by about ten-fold higher sedimentation rates.

Supplementary material related to this article is available online at:
<http://www.clim-past-discuss.net/9/3061/2013/cpd-9-3061-2013-supplement.pdf>.

Acknowledgements. Funding for this research was provided by the International Continental Scientific Drilling Program (ICDP), the US National Science Foundation (NSF), the German Federal Ministry of Education and Research (BMBF), Alfred Wegener Institute (AWI) and Helmholtz Centre Potsdam (GFZ), the Russian Academy of Sciences Far East Branch (RAS FEB), the Russian Foundation for Basic Research (RFBR), and the Austrian Federal Ministry of Science and Research (BMWF). The Russian GLAD 800 drilling system was developed and operated by DOSECC Inc., the down hole logging was performed by the ICDP-OSG, and LacCore, at the University of Minnesota, handled core curation. We like to thank all the participants of the expedition to Lake El'gygytyn from January to May 2009 for their engagement during recovery of the ICDP Site 5011-1 cores. Numerous students helped during laboratory work. This study was partly financed by BMBF grant no. 03G0642C – “Geochronology of the sediments in the El'gygytyn crater”.

The service charges for this open access publication have been covered by a Research Centre of the Helmholtz Association.

Chronology of Lake El'gygytyn sediments

N. R. Nowaczyk et al.

Title Page

Abstract

Introduction

Conclusions

References

Tables

Figures



Back

Close

Full Screen / Esc

Printer-friendly Version

Interactive Discussion



References

- Andreev, A. A., Tarasov, P. E., Rashke (Morozova), E., Wennrich, V., Nowaczyk, N. R., Brigham-Grette, J., and Melles, M.: Late Pliocene/Early Pleistocene environments of the north-eastern Siberian Arctic inferred from Lake El'gygytyn pollen record, *Clim. Past*, 201.
- 5 Berger, A. and Loutre, M. F.: Insolation values for the climate of the last 10 million of years, *Quaternary Sci. Rev.*, 10, 297–317, 1991.
- Blaauw, M.: Out of tune: the dangers of aligning proxy archives, *Quaternary Sci. Rev.*, 36, 38–49, 2012.
- Bokhorst, M. P. and Vandenberghe, J.: Validation of wiggle matching using a multi-proxy approach and its palaeoclimatic significance, *J. Quaternary Sci.*, 24, 937–947, 2009.
- 10 Brigham-Grette, J., Melles, M., Minyuk, P., Andreev, A., Tarasov, P., DeConto, R., Koenig, S., Nowaczyk, N., Wennrich, V., Rosén, P., Haltia, E., Cook, T., Gebhard, C., Meyer-Jacob, C., Snyder, J., and Herzschuh, U.: Pliocene warmth, polar amplification, and stepped Pleistocene cooling recorded in NE Arctic Russia, *Science express*, doi:10.1126/science.1233137, in press, 2013.
- 15 Channell, J. E. T., Mazaud, A., Sullivan, P., Turner, S., and Raymo, M. E.: Geomagnetic excursions and paleointensities in the Matuyama Chron at Ocean Drilling Program Sites 983 and 984 (Iceland Basin), *J. Geophys. Res.*, 107, doi:10.1029/2001JB000491, 2002.
- Channell, J. E. T., Lubs, J., and Raymo, M. E.: The Réunion subchronozone at ODP site 981 (Feni Drift, North Atlantic), *Earth Planet. Sci. Lett.*, 215, 1–12, 2003.
- 20 Channell, J. E. T., Xuan, C., and Hodell, D. A.: Stacking paleointensity and oxygen isotope data for the last 1.5 Myr (PISO-1500), *Earth Planet. Sci. Lett.*, 283, 14–23, 2009.
- Cherapanova, M. V., Snyder, J. A., and Brigham-Grette, J.: Diatom stratigraphy of the last 250 ka at Lake El'gygytyn, northeast Siberia, *J. Paleolimnol.*, 37, 155–162, 2007.
- 25 Deino, A. L., Kingston, J. D., Glen, J. M., Edgar, R. K., and Hill, A.: Precessional forcing of lacustrine sedimentation in the late Cenozoic Chemeron Basin, Central Kenya Rift, and calibration of the Gauss/Matuyama boundary, *Earth Planet. Sci. Lett.*, 247, 41–60, 2006.
- Frank, U., Nowaczyk, N. R., Minyuk, P., Vogel, H., Rosén, P., and Melles, M.: A 350 kyr record of climate change from Lake El'gygytyn, Far East Russian Arctic: refining the pattern of climate modes by means of cluster analysis, *Clim. Past Discuss.*, 8, 5109–5132, doi:10.5194/cpd-8-5109-2012, 2012.
- 30

Chronology of Lake El'gygytyn sediments

N. R. Nowaczyk et al.

Title Page

Abstract

Introduction

Conclusions

References

Tables

Figures

◀

▶

◀

▶

Back

Close

Full Screen / Esc

Printer-friendly Version

Interactive Discussion



Chronology of Lake El'gygytyn sediments

N. R. Nowaczyk et al.

Title Page

Abstract

Introduction

Conclusions

References

Tables

Figures

◀

▶

◀

▶

Back

Close

Full Screen / Esc

Printer-friendly Version

Interactive Discussion

- Francke, A., Wennrich, V., Sauerbrey, M., Juschus, O., Melles, M., and Brigham-Grette, J.: Multivariate statistic and time series analyses of grain-size data in Quaternary sediments of Lake El'gygytyn, NE Russia, *Clim. Past Discuss.*, 9, 217–244, doi:10.5194/cpd-9-217-2013, 2013.
- 5 Guo, B., Zhu, R., Florindo, F., Ding, Z., and Sun, J. A.: A short, reverse polarity interval within the Jaramillo subchron: Evidence from the Jingbian section, northern China Loess plateau, *J. Geophys. Res.*, 107, 10029–10040, 2002.
- Gurov, E. P. and Koeberl, C.: Shocked rocks and impact glasses from the El'gygytyn impact structure, Russia, *Meteorit. Planet. Sci.*, 39, 1495–1508, 2004.
- 10 Haltia, E. M. and Nowaczyk, N. R.: Magnetostratigraphy of sediments from Lake El'gygytyn ICDP site 5011-1: paleomagnetic age constraints for the longest continental record from the Arctic, *Clim. Past*, in preparation, 2013.
- Hunt, R. W.: *Measuring colour*, 3rd Ed., Founta in Press, England, 1998.
- Juschus, O., Preusser, F., Melles, M., and Radtke, U.: Applying SAR-IRSL methodology for dating fine-grained sediments from Lake El'gygytyn, north-eastern Siberia, *Quaternary Geochron.*, 2, 187–194, 2007.
- 15 Kirschvink, J. L.: The least-squares line and plane and the analysis of palaeomagnetic data, *Geophys. J. R. Astr. Soc.*, 62, 699–718, 1980.
- Kelley, S. P., Spicer, R. A., and Herman, A. B.: New $^{40}\text{Ar}/^{39}\text{Ar}$ dates for Cretaceous Chauna Group tephra, north-eastern Russia, and their implications for the geologic history and floral evolution of the North Pacific region, *Cret. Res.*, 20, 97–106, 1999.
- 20 Laj, C. and Channell, J. E. T.: Geomagnetic excursions, in: *Treatise on Geophysics*, edited by: Schubert, G., Bercovici, D., Dziewonski, A., Herring, T., Kanamori, H., Kono, M., Olson, P. L., Price, G. D., Romanowicz, B., Spohn, T., Stevenson, D., and Watts, A. B., *Geomagnetism*, 5. Elsevier, B.V., Amsterdam, 373–416, 2007.
- 25 Laskar, J., Robutel, F., and Boudin, F.: Orbital, precessional, and insolation quantities for the Earth from –20 Myr to +10 Myr, *Astron. Astrophys.*, 270, 522–533, 1993.
- Laskar, J., Robutel, P., Joutel, F., Gastineau, M., Correia, A. C. M., and Levrard, B.: A long-term numerical solution for the insolation quantities of the Earth, *Astron. Astrophys.*, 428, 261–285, 2004.
- 30 Layer, P.W.: Argon-40/Argon-39 age of the El'gygytyn impact event, Chukotka, Russia, *Meteorit. Planet. Sci.*, 35, 591–599, 2000.

Chronology of Lake El'gygytyn sediments

N. R. Nowaczyk et al.

Title Page

Abstract

Introduction

Conclusions

References

Tables

Figures



Back

Close

Full Screen / Esc

Printer-friendly Version

Interactive Discussion

- Milankovitch, M.: Kanon der Erdbestrahlung und seine Anwendung auf das Eiszeitenproblem, Königlich Serbische Akademie, Belgrad, 633 pp., 1941.
- Minyuk, P. S., Brigham-Grette, J., Melles, M., Borkhodoev, V. Y., and Glushkova, O. Y.: Inorganic geochemistry of El'gygytyn Lake Sediments (northeastern Russia) as an indicator of paleoclimatic change for the last 250 kyr, *J. Paleolimnol.*, 37, 123–133, 2007.
- Murdock, K. J., Wilkie, K., and Brown, L. L.: Rock magnetic properties, magnetic susceptibility, and organic geochemistry comparison in core LZ1029-7 Lake El'gygytyn, Russia Far East, *Clim. Past*, 9, 467–479, doi:10.5194/cp-9-467-2013, 2013.
- Nolan, M. and Brigham-Grette, J.: Basic hydrology, limnology, and meteorology of modern Lake El'gygytyn, Siberia, *J. Paleolimnol.*, 37, 17–35, 2007.
- Nowaczyk, N. R.: Logging of magnetic susceptibility, in: Tracking environmental change using lake sediments, Vol I: Basin analysis, coring, and chronological techniques, edited by: Last, W. M. and Smol, J. P., Kluwer Academic Publishers, Bortrecht, Netherlands, 155–170, 2001.
- Nowaczyk, N. R., Minyuk, P., Melles, M., Brigham-Grette, J., Glushkova, O., Nolan, M., Lozhkin, A. V., Stetsenko, T. V., Anderson, P. M., and Forman, S. L.: Magnetostratigraphic results from impact crater Lake El'gygytyn, northeastern Siberia: a 300 kyr long high-resolution terrestrial palaeoclimatic record from the Arctic, *Geophys. J. Int.*, 150, 109–126, 2002.
- Nowaczyk, N. R., Melles, M., and Minyuk, P.: A revised age model for core PG1351 from Lake El'gygytyn, Chukotka, based on magnetic susceptibility variations tuned to northern hemisphere insolation variations, *J. Paleolimnol.*, 37, 65–76, 2007.
- Ogg, J. G. and Smith, A. G.: The geomagnetic polarity time scale, in: A Geological Timescale 2004, edited by: Gradstein, F., Ogg, J., and Smith, A., Cambridge University Press, 63–86, 2004.
- Prokopenko, A. A. and Khursevich, G. K.: Plio-Pleistocene transition in the continental record from Lake Baikal: Diatom biostratigraphy and age model, *Quaternary Int.*, 219, 26–36. 2010.
- Prokopenko, A. A., Hinnov, L. A., Williams, D. F., and Kuzmin, M. I.: Orbital forcing of continental climate during the Pleistocene: a complete astronomically tuned climatic record from Lake Baikal, SE Siberia, *Quaternary Sci. Rev.*, 25, 3431–3457, 2006.
- Quidelleur, X., Holt, J. W., Salvany, T., and Bouquerel, H.: New K-Ar ages from La Montagne massif, Réunion Island (Indian Ocean), supporting two geomagnetic events in the time period 2.2–2.0 Ma, *Geophys. J. Int.*, 182, 699–710, 2010.
- Rosén, P., Vogel, H., Cunningham, L., Reuss, N., Conley, D. J., and Persson, P.: Fourier transform infrared spectroscopy, a new method for rapid determination of total organic and

Chronology of Lake El'gygytyn sediments

N. R. Nowaczyk et al.

[Title Page](#)[Abstract](#)[Introduction](#)[Conclusions](#)[References](#)[Tables](#)[Figures](#)[Back](#)[Close](#)[Full Screen / Esc](#)[Printer-friendly Version](#)[Interactive Discussion](#)

inorganic carbon and biogenic silica concentration in lake sediments, *J. Paleolimnol.*, 43, 247–259, 2010.

Rosén, P., Vogel, H., Cunningham, L., Hahn, A., Hausmann, S., Pienitz, R., Zolitschka, B., Wagner, B., and Persson, P.: Universally applicable model for the quantitative determination of lake sediment composition using Fourier transform infrared spectroscopy, *Environ. Sci. Technol.*, 45, 8858–8865, 2011.

Sauerbrey, M. A., Juschus, O., Gebhardt, A. C., Wennrich, V., Nowaczyk, N. R., and Melles, M.: Mass movement deposits in the 3.6 Ma sediment record of Lake El'gygytyn, Far East Russian Arctic: classification, distribution and preliminary interpretation, *Clim. Past Discuss.*, 9, 467–505, doi:10.5194/cpd-9-467-2013, 2013.

Singer, B. A., Brown, L. L., Rabassa, J. O., and Guillou, H.: $^{40}\text{Ar}/^{39}\text{Ar}$ chronology of Late Pliocene and Early Pleistocene geomagnetic and glacial events in Southern Argentina, in: *Timescales of the Paleomagnetic Field*, edited by: Channell, J. E. T., Kent, D. V., Lowrie, W., and Meert, J. G., *Geophys. Monograph Ser.*, 145, Amer. Geophys. Union, Washington, D.C., 175–190, 2004.

Vogel, H., Rosén, P., Wagner, B., Melles, M., and Persson, P.: Fourier transform infrared spectroscopy, a new cost-effective tool for quantitative analysis of biogeochemical properties in long sediment records, *J. Paleolimnol.*, 40, 689–702, 2008.

Vogel, H., Meyer-Jacob, C., Melles, M., Brigham-Grette, J., Andreev, A. A., Wennrich, V., and Rosén, P.: Detailed insight into Arctic climatic variability during MIS 11 at Lake El'gygytyn, NE Russia, *Clim. Past Discuss.*, 8, 6309–6339, doi:10.5194/cpd-8-6309-2012, 2012.

Wennrich, V., Minyuk, P., Borkhodoev, V., Francke, A., Ritter, B., Raschke, U., Nowaczyk, N., Schwamborn, G., Brigham-Grette, J., and Melles, M.: Pliocene to Pleistocene climate and environmental history of lake El'gygytyn/ NE Russia based on high-resolution inorganic geochemistry data, *Clim. Past.*, in preparation, 2013.

Yamazaki, T. and Oda, H.: A geomagnetic paleointensity stack between 0.8 and 3.0 Ma from equatorial Pacific sediment cores, *Geochem. Geophys. Geosyst.*, 6, Q11H20, doi:10.1029/2005GC001001, 2005.

Chronology of Lake El'gygytyn sediments

N. R. Nowaczyk et al.

Title Page

Abstract

Introduction

Conclusions

References

Tables

Figures

◀

▶

◀

▶

Back

Close

Full Screen / Esc

Printer-friendly Version

Interactive Discussion



Table 1. Ages of geomagnetic reversals from various authors, listed in the first row, and as inferred from multi-proxy tuning of ICDP Site 5011-1 sediments from lake El'gygytyn in this study, listed in the right column. Here, bold numbers indicate new/alternative ages, otherwise ages were adopted from Liesiecki and Raymo (2005).

Authors	Cande and Kent (1995)	Lourens et al. (1996)	Ogg and Smith (2004)	Lisiecki and Raymo (2004)	This study
	Age				
Reversal subchron <i>cryptochron/excursion</i>	Ma	Ma	Ma	Ma	Ma
Brunhes/Matuyama	0.780		0.781	0.780	0.780
Jaramillo (t)	0.990		0.988	0.991	0.991
<i>intra-Jaramillo excursion (t)</i>					1.0142
<i>intra-Jaramillo excursion (o)</i>					1.0192
Jaramillo (o)	1.070		1.072	1.075	1.075
<i>Cobb-Mountain (t)</i>	1.201		1.173		1.1858
<i>Cobb-Mountain (o)</i>	1.211		1.185		1.1938
Olduvai (t)	1.770	1.785	1.778	1.781	1.781
Olduvai (o)	1.950	1.942	1.945	1.968	1.968
<i>Olduvai precursor (t)</i>					1.9782
<i>Olduvai precursor (o)</i>					1.9815
<i>La Réunion (t)</i>	2.140	2.129	2.128		2.1216
<i>La Réunion (o)</i>	2.150	2.149	2.148		2.1384
Matuyama/Gauss	2.581	2.582	2.581	2.608	2.588
Kaena (t)	3.040	3.032	3.032	3.045	3.045
Kaena (o)	3.110	3.116	3.116	3.127	3.127
Mammoth (t)	3.220	3.207	3.207	3.210	3.210
Mammoth (o)	3.330	3.330	3.330	3.319	3.319
Gauss/Gilbert	3.580	3.596	3.596	3.588	3.588

Here: t – termination, o – onset.

Chronology of Lake El'gygytyn sediments

N. R. Nowaczyk et al.

Table 2. Overview of stratigraphic data used for multi-proxy tuning of Lake El'gygytyn sediments: number of obtained logger readings or individual determinations, with numbers in italics indicating raw data that was acquired on the full stratigraphic lengths of the respective cores. Scanning/sampling intervals are given below the parameter notation.

Data set	5011-1A	5011-1B	5011-1C	5011 comp.	Lz1024	PG1351	Total
MS2E ⁽¹⁾ 1 mm	<i>122 939</i>	<i>100 606</i>	<i>95 264</i>	143 752	16 026	11 050	489 637
Color ⁽²⁾ 1 mm	<i>122 988</i>	<i>101 074</i>	<i>99 060</i>	138 623	no	no	461 745
XRF ⁽³⁾ 2 mm	<i>61 357</i>	<i>50 132</i>	<i>46 464</i>	71 263	8273	186	237 675
NRM, ChRM ⁽⁴⁾ 2 (10–15) cm	<i>5806</i>	<i>4848</i>	<i>2113</i>	5883	607	476	19 733
biog. Silica ⁽⁵⁾ (1) 2 cm	<i>no</i>	<i>no</i>	<i>no</i>	5856	1657	229	7742
TOC ⁽⁶⁾ (1) 2 cm	<i>no</i>	<i>no</i>	<i>no</i>	6136	1658	334	7847
grain size 8 cm	<i>no</i>	<i>no</i>	<i>no</i>	1125	no	no	1125
Tree pollen ⁽⁷⁾ 5–6 (30–300) cm				392	184	124	556

⁽¹⁾ magnetic susceptibility, ⁽²⁾ full visible colour spectrum (36 lines), (X,Y,Z) tristimulus values, (L*,a*,b*), hue angle,

⁽³⁾ X-ray fluorescence spectra, abundance of major elements, ⁽⁴⁾ natural remanent magnetisation (NRM) and characteristic remanent magnetisation (ChRM) from U-channels, sampling interval for discrete samples in brackets,

⁽⁵⁾ from Fourier Transform Infrared Spectroscopy (FTIRS-BSi), sampling interval for Lz1024 in brackets,

⁽⁶⁾ total organic carbon, sampling interval for Lz1024 in brackets, ⁽⁷⁾ sampling interval for Pliocene interval in ICDP Site 5011-1 cores in brackets.

Title Page

Abstract

Introduction

Conclusions

References

Tables

Figures

⏪

⏩

◀

▶

Back

Close

Full Screen / Esc

Printer-friendly Version

Interactive Discussion



Chronology of Lake El'gygytyn sediments

N. R. Nowaczyk et al.

Table 3. Positions and ages of tephra layers identified in lake El'gygytyn sediments. Core labels indicate: 1 – PG1351, 2 – Lz1024, A – 5011-1A, B – 5011-1B, C – 5011-1C.

Core	Index	5011-1 composite depth (m)	Age (ka)
1, 2	0	2.54–2.55	58
1, 2, A, B	1	7.88–7.89	177
A, B	2	27.52–27.52	674
A, B	3	36.41–36.47	918
A, B	4	60.79–60.80	1411
A, B	5	62.04–62.08	1434
A, B	6	79.25–79.26	1775
A, B, C	7	104.93–105.00	2225

[Title Page](#)
[Abstract](#)
[Introduction](#)
[Conclusions](#)
[References](#)
[Tables](#)
[Figures](#)

[Back](#)
[Close](#)
[Full Screen / Esc](#)
[Printer-friendly Version](#)
[Interactive Discussion](#)


Chronology of Lake El'gygytyn sediments

N. R. Nowaczyk et al.

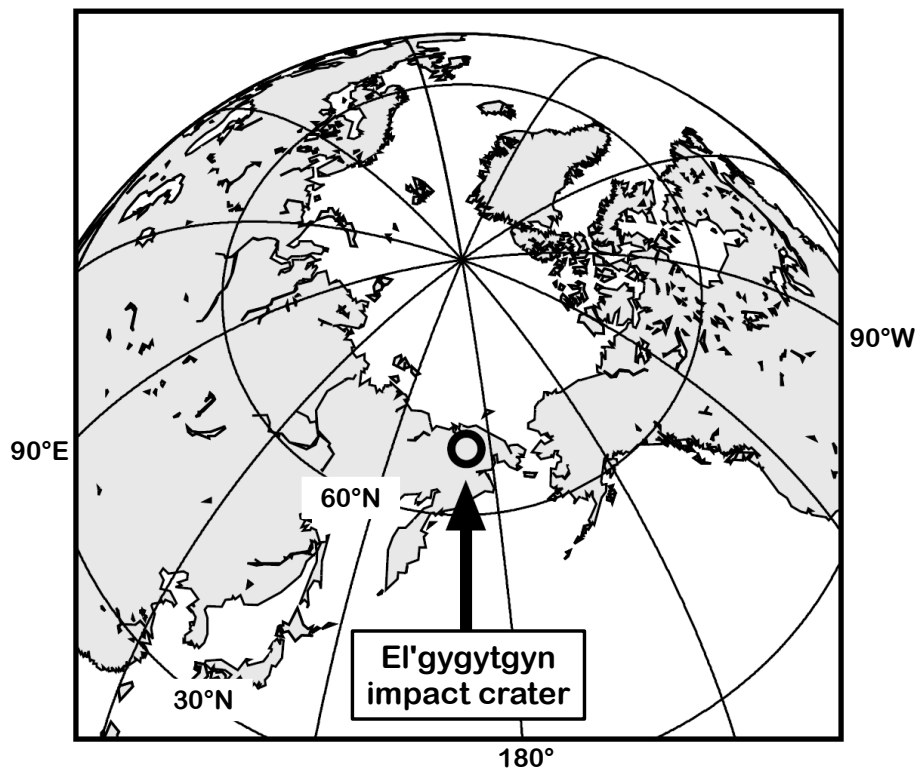


Fig. 1. Location of Lake El'gygytyn in the Far Eastern Russian Arctic. The circle (not to scale) marks the site of the impact crater.

[Title Page](#)[Abstract](#)[Introduction](#)[Conclusions](#)[References](#)[Tables](#)[Figures](#)[◀](#)[▶](#)[◀](#)[▶](#)[Back](#)[Close](#)[Full Screen / Esc](#)[Printer-friendly Version](#)[Interactive Discussion](#)

Chronology of Lake El'gygytyn sediments

N. R. Nowaczyk et al.

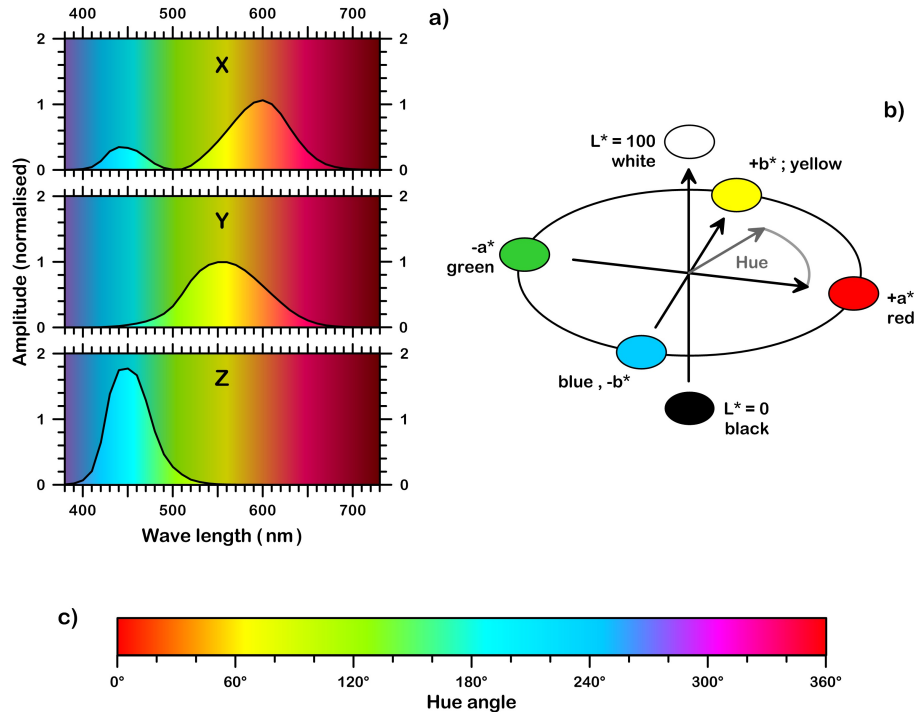


Fig. 2. Some basics in color processing: **(a)** 2° -observer weighting functions for spectrum integration in order to obtain the tristimulus values (X,Y,Z), **(b)** $L^*a^*b^*$ color space and definition of the hue angle as also shown in **(c)**, together with corresponding colors. Note that colors are more schematic rather than realistic.

[Title Page](#)
[Abstract](#)
[Introduction](#)
[Conclusions](#)
[References](#)
[Tables](#)
[Figures](#)
[Back](#)
[Close](#)
[Full Screen / Esc](#)
[Printer-friendly Version](#)
[Interactive Discussion](#)

Chronology of Lake El'gygytyn sediments

N. R. Nowaczyk et al.

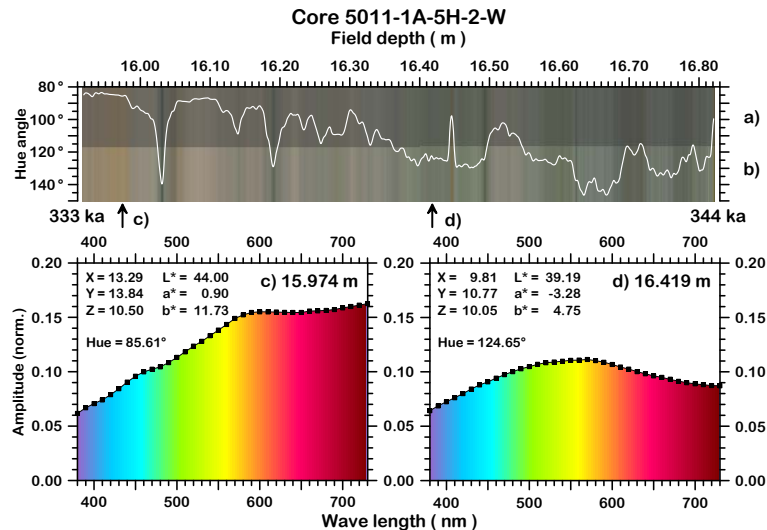


Fig. 3. Example for quantitative color data acquisition from core 5011-1A-5H-W in field depth across Termination IV (time interval from 344 to 333 ka): **(a)** original and **(b)** contrast-enhanced down-core variation of colors measured with a GretagMacbeth Spectrolino™ spectrophotometer, together with hue angle (white curve), **(c)** and **(d)** two individual spectra including tristimulus values (X,Y,Z), (L*,a*,b*) values, hue angle (see Fig. 2), and logging depth. The positions of the two measuring points are marked by arrows below **(b)**.

Title Page

Abstract

Introduction

Conclusions

References

Tables

Figures

◀

▶

◀

▶

Back

Close

Full Screen / Esc

Printer-friendly Version

Interactive Discussion



Chronology of Lake El'gygytyn sediments

N. R. Nowaczyk et al.

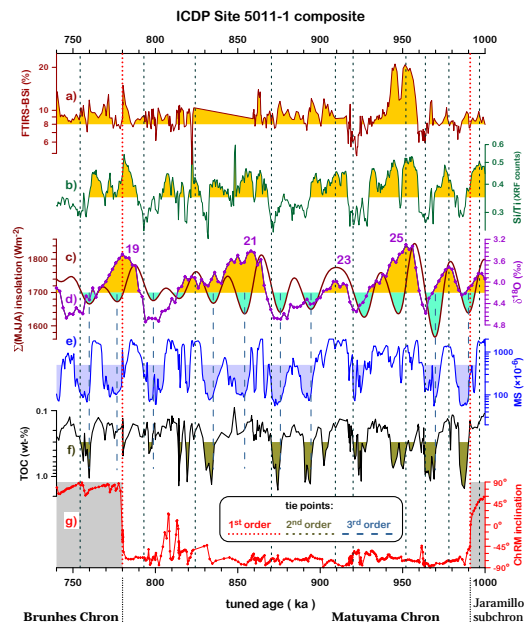


Fig. 4. Definition of 1st, 2nd, and 3rd order tie points of the age model: Chronostratigraphic plot for the time window 740 to 1000 ka of **(a)** biogenic silica (FTIRS-BSi), **(b)** Si/Ti-ratio, with high (low) ratios indicating higher (lower) biogenic input with respect to lithogenic input, **(c)** cumulative summer (May to August) insolation for 67.5° N (according to Laskar et al., 2004), **(d)** LR04 oxygen isotope stack ($\delta^{18}\text{O}$) from Lisiecki and Raymo (2005), **(e)** magnetic susceptibility (MS), **(f)** total organic carbon (TOC), and **(g)** ChRM inclination, with grey (white) indicating normal (reversed) polarity. Geomagnetic field reversals are defined as 1st order tie points of the age model. Correlation of Si/Ti-ratio and biogenic silica to the LR04 stack define 2nd order tie points, and correlation of magnetic susceptibility and TOC to insolation patterns define 3rd order tie points. For further details, see text. FTIRS – Fourier transform infrared spectroscopy, XRF – X-ray fluorescence, ChRM – Characteristic Remanent Magnetization.

Chronology of Lake El'gygytyn sediments

N. R. Nowaczyk et al.

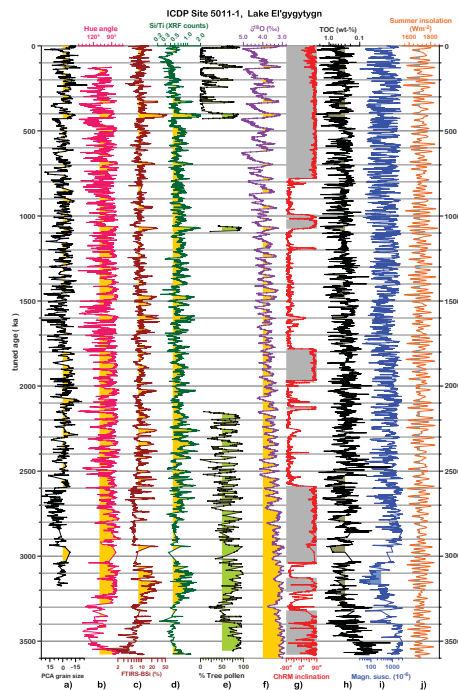


Fig. 5. Chrono-stratigraphic plot of main parameters used for developing the age model of the ICDP Site 5011-1 composite record from Lake El'gygytyn: **(a)** grain size data from principle component analysis (PCA), with negative (positive) values representing coarse (fine) grained sediments, **(b)** hue angle from photospectrometry (see Fig. 2), **(c)** biogenic silica from Fourier transform infrared spectroscopy (FTIRS-BSi), **(d)** Si/Ti-ratio from X-ray fluorescence (XRF) scanning, **(e)** Tree and shrub pollen percentages, **(f)** marine oxygen isotope stack (Lisiecki and Raymo, 2005), **(g)** inclination of the characteristic remanent magnetisation (ChRM), with grey (white) indication normal (reversed) polarity, **(h)** total organic carbon (TOC), **(i)** magnetic susceptibility, and **(j)** the cumulative Northern Hemisphere summer insolation (May to August), according to orbital solutions provided by (Laskar et al., 2004).

[Title Page](#)
[Abstract](#)
[Introduction](#)
[Conclusions](#)
[References](#)
[Tables](#)
[Figures](#)

[Back](#)
[Close](#)
[Full Screen / Esc](#)
[Printer-friendly Version](#)
[Interactive Discussion](#)


Chronology of Lake El'gygytyn sediments

N. R. Nowaczyk et al.

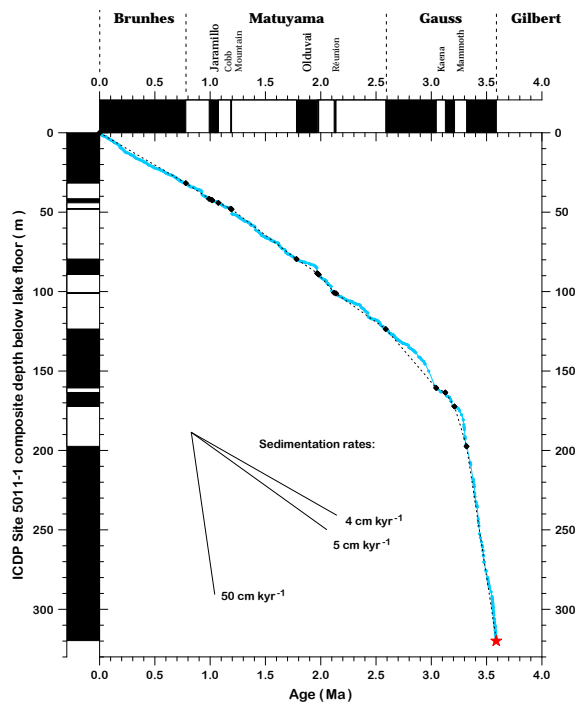


Fig. 6. Age depth model for the ICDP Site 5011-1 sedimentary composite record derived from tuning of physical, sedimentological, geochemical, and pollen records to the benthic oxygen isotope stack from Lisiecki and Raymo (2005) and the Northern summer insolation according to orbital solutions provided by (Laskar et al., 2004), respectively. Initial 1st order tie points (black diamonds) were provided by a comprehensive magnetostratigraphic investigation of ICDP Site 5011-1 cores (Haltia and Nowaczyk, 2013; see also Fig. 2). The red star marks the time of the impact inferred from $^{40}\text{Ar}/^{39}\text{Ar}$ dating (Layer, 2000) at $3.58 (\pm 0.04)$ ka. Black (white) denote normal (reversed) polarity.

Title Page

Abstract

Introduction

Conclusions

References

Tables

Figures



Back

Close

Full Screen / Esc

Printer-friendly Version

Interactive Discussion



Chronology of Lake El'gygytyn sediments

N. R. Nowaczyk et al.

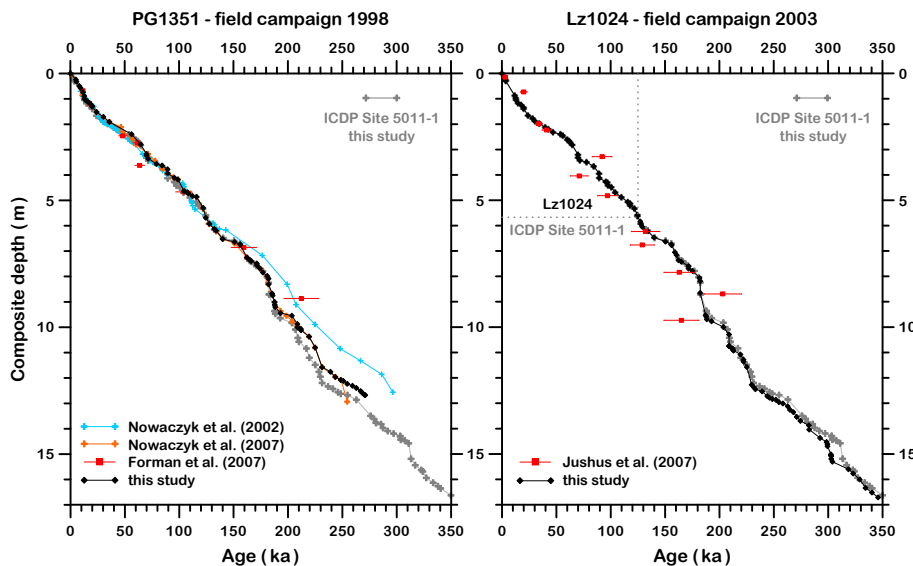


Fig. 7. Age depth models for pilot cores PG1351 (1998) and Lz1024 (2003) after synchronizing with ICDP Site 5011-1 age model (Fig. 6). Red squares with error bars mark results from infrared stimulated luminescence (IRSL) dating. The dotted line in the right graph mark the junction between Lz1024 and the ICDP Site 5011-1 composite record, assembled from cores 5011-1A, -1B, and -1C.

[Title Page](#)
[Abstract](#)
[Introduction](#)
[Conclusions](#)
[References](#)
[Tables](#)
[Figures](#)

[Back](#)
[Close](#)
[Full Screen / Esc](#)
[Printer-friendly Version](#)
[Interactive Discussion](#)


Chronology of Lake El'gygytyn sediments

N. R. Nowaczyk et al.

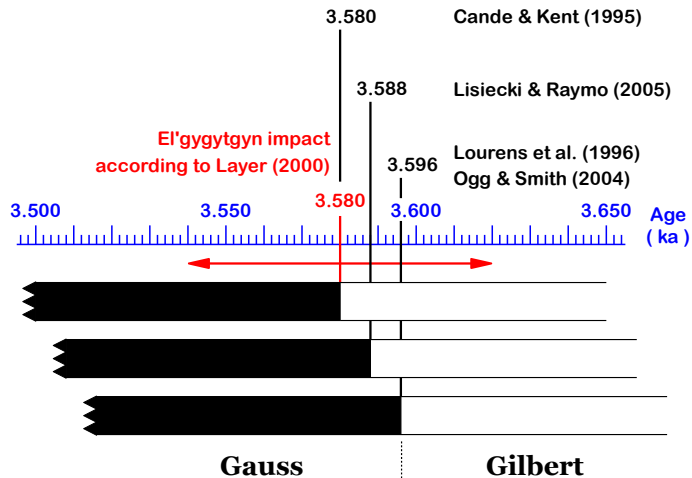


Fig. 8. Radiometric dating of the El'gygytyn impact (Layer, 2000) in the context of currently used geomagnetic polarity time scales. Since the lowermost ICDP Site 5011-1 sediments show clear normal polarity directions, the impact must have occurred after the Gilbert Gauss reversal.

Title Page

Abstract

Introduction

Conclusions

References

Tables

Figures

⏪

⏩

◀

▶

Back

Close

Full Screen / Esc

Printer-friendly Version

Interactive Discussion



Chronology of Lake El'gygytyn sediments

N. R. Nowaczyk et al.

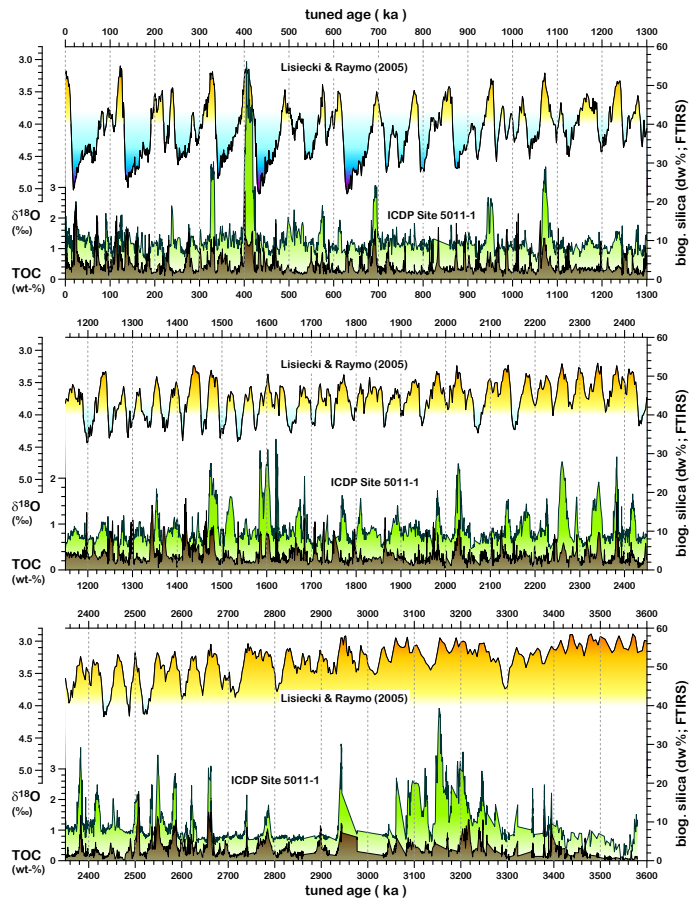


Fig. 9a. Caption on p. 3102.

Title Page

Abstract

Introduction

Conclusions

References

Tables

Figures



Back

Close

Full Screen / Esc

Printer-friendly Version

Interactive Discussion



Chronology of Lake El'gygytyn sediments

N. R. Nowaczyk et al.

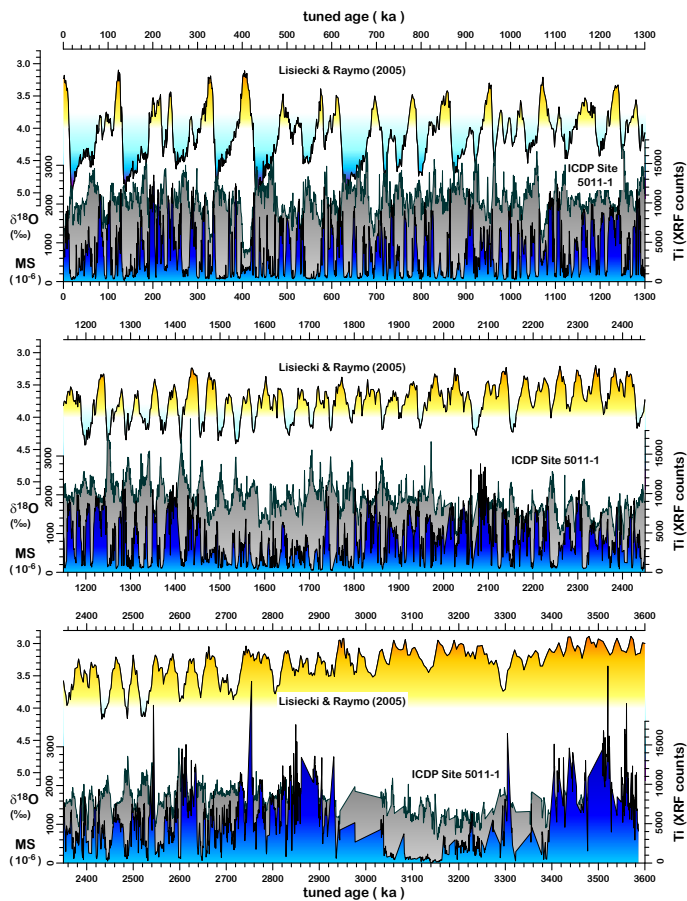


Fig. 9b. Caption on p. 3102.

Title Page

Abstract

Introduction

Conclusions

References

Tables

Figures



Back

Close

Full Screen / Esc

Printer-friendly Version

Interactive Discussion



Chronology of Lake El'gygytyn sediments

N. R. Nowaczyk et al.

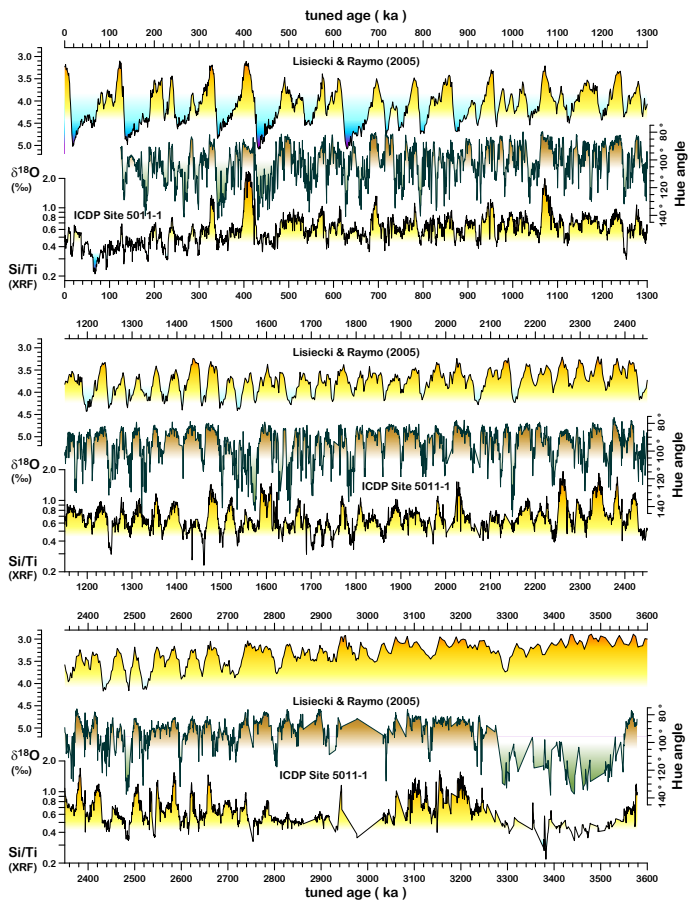


Fig. 9c. Caption on p. 3102.

Title Page

Abstract

Introduction

Conclusions

References

Tables

Figures



Back

Close

Full Screen / Esc

Printer-friendly Version

Interactive Discussion



Chronology of Lake El'gygytgyn sediments

N. R. Nowaczyk et al.

Fig. 9. Response of Lake El'gygytgyn (ICDP Site 5011-1) to climate variability as represented by the marine oxygen isotope ($\delta^{18}\text{O}$) stack LR04 (Lisiecki and Raymo, 2005): time series of **(a)** biogenic silica (FTIRS estimation), representing bioproductivity in the upper water layers of the lake, and total organic carbon (TOC), representing preservation of organic matter at the lake floor during phases of anoxic bottom waters, **(b)** Ti content (XRF counts), taken as a proxy of lithogenic input from the catchment, and magnetic susceptibility (MS), representing preservation of magnetic particles during phases of oxygenated bottom waters, **(c)** hue angle (color) and Si/Ti-ratio, both following global climate cycles. Curves in **(a)** and **(b)** were plotted in a way that TOC (MS) superimposes biogenic silica (Ti) in time intervals when best preservation of organic matter (magnetic particles) can be assumed during anoxic (oxic) conditions at the lake floor. Where the TOC curve lies below the biogenic silica curve in **(a)**, partial degradation (60 to 80 %) of organic matter is indicated (green area between both curves). Where the MS curve lies below the Ti curve in **(b)**, fairly massive dissolution (up to 95 %) of the magnetic fraction in the sediments is indicated (grey area between both curves). For further explanation see discussion in the text.

[Title Page](#)[Abstract](#)[Introduction](#)[Conclusions](#)[References](#)[Tables](#)[Figures](#)[Back](#)[Close](#)[Full Screen / Esc](#)[Printer-friendly Version](#)[Interactive Discussion](#)